Comparison of public codes for Drell-Yan processes at NNLO accuracy

Zoltán Trócsányi

with Sergey Alekhin, Adam Kardos and Sven-Olaf Moch

Eötvös University and MTA-DE Particle Physics Research Group

based on arXiv:2104.02400 (EPJC)

HEP2021

VIRTUAL EDITION

July 29, 2021

Motto: precise measurements require precise theoretical predictions

- Experimental fiducial measurements of Drell-Yan cross-sections have now reached <0.5% accuracy — apart from the luminosity uncertainty arXiv:1612.03016 (ATLAS), arXiv: 1909.0413 (CMS)

	$\sigma^{\text{fid}}_{W\to\ell\nu}$ [pb]
$W^+ \to e^+\nu$	2939 ± 1 (stat) ± 28 (syst) ± 53 (lumi)
$W^+ \to \mu^+\nu$	2948 ± 1 (stat) ± 21 (syst) ± 53 (lumi)
$W^+ \to \ell^+\nu$	2947 ± 1 (stat) ± 15 (syst) ± 53 (lumi)
$W^- \to e^-\bar{\nu}$	1957 ± 1 (stat) ± 21 (syst) ± 35 (lumi)
$W^- \to \mu^-\bar{\nu}$	1964 ± 1 (stat) ± 13 (syst) ± 35 (lumi)
$W^- \to \ell^-\bar{\nu}$	1964 ± 1 (stat) ± 11 (syst) ± 35 (lumi)
$W \to e\nu$	4896 ± 2 (stat) ± 49 (syst) ± 88 (lumi)
$W \to \mu\nu$	4912 ± 1 (stat) ± 32 (syst) ± 88 (lumi)
$W \to \ell\nu$	4911 ± 1 (stat) ± 26 (syst) ± 88 (lumi)
	$\sigma^{\text{fid}}_{Z/\gamma^*\to\ell\ell}$ [pb]
$Z/\gamma^* \to e^+e^-$	502.7 ± 0.5 (stat) ± 2.0 (syst) ± 9.0 (lumi)
$Z/\gamma^* \to \mu^+\mu^-$	501.4 ± 0.4 (stat) ± 2.3 (syst) ± 9.0 (lumi)
$Z/\gamma^* \to \ell\ell$	502.2 ± 0.3 (stat) ± 1.7 (syst) ± 9.0 (lumi)

ATLAS fiducial cross sections at 7 TeV in the 66 < m_{ll}/GeV < 116 mass window

Motto: precise measurements require precise theoretical predictions

- Experimental fiducial measurements of Drell-Yan cross-sections have now reached <0.5% accuracy — apart from the luminosity uncertainty (ATLAS: 1612.03016, CMS: 1909.0413)
- QCD fixed-order predictions agree in full phase space
- but they differ at NNLO by as much as 1% in fiducial regions with symmetric cuts on the leptons

Data sets

Not necessary, but helpful, so chose two sets of data

- ATLAS data at E_{cm} = 7 TeV as pseudorapidity distributions for the arXiv:1612.03016
  - decay electron or muon ($W^{\pm}$-production) and
  - decay lepton- pair (Z/γ^{*}-production)
  - transverse momenta p_T and the pseudo-rapidities η_l of the decay leptons are subject to fiducial cuts

- DØ data E_{cm} = 1.96 TeV on $W^{\pm}$-production arXiv:1412.2862
  - measures the electron charge asymmetry distributions
  - and their dependence on the electron pseudo-rapidity
  - both symmetric as well as staggered fiducial cuts are applied on the transverse momenta and pseudo-rapidities of the electron and the neutrino

Parameters

Important for precision comparison

- G_μ scheme with input values G_F, M_Z, M_W ($\sin^2\theta_w$, $\alpha(M_Z)$ are output), which minimizes the impact of NLO electroweak corrections

$$G_\mu = 1.16637 \times 10^{-5}\ \mathrm{GeV}^{-2},$$
$$M_Z = 91.1876\ \mathrm{GeV}, \qquad \Gamma_Z = 2.4952\ \mathrm{GeV},$$
$$M_W = 80.379\ \mathrm{GeV}, \qquad \Gamma_W = 2.085\ \mathrm{GeV},$$

$$\begin{aligned}
|V_{ud}| &= 0.97401, & |V_{us}| &= 0.2265\ \ , \\
|V_{cd}| &= 0.2265\ \ , & |V_{cs}| &= 0.97320, \\
|V_{ub}| &= 0.00361, & |V_{cb}| &= 0.04053.
\end{aligned}$$

- $\overline{\mathrm{MS}}$ factorization scheme with $n_f = 5$ light flavors
- ABMP16 PDF with $\alpha^{(5)}(M_Z) = 0.1147$, $\mu_R = \mu_F = M_V$

Public codes

- DYNNLO (version 1.5) http://theory.fi.infn.it/grazzini/dy.html
  uses q_T-subtraction
- FEWZ (version 3.1) https://www.hep.anl.gov/fpetriello/FEWZ.html
  uses fully local subtraction scheme
- MATRIX (version 1.0.4) https://matrix.hepforge.org/
  uses q_T-subtraction and scattering amps from OpenLoops
- MCFM (version 9.0) https://mcfm.fnal.gov/
  uses N-jettiness subtraction
- Slicing parmeters:
  - r_{cut} for MATRIX as a cut on q_T
  - τ_{cut} for MCFM on jettiness

Validation at LO and NLO

- Consistency of parameters: agreement at $O(10^{-5})$ at LO

Validation at LO and NLO

- Consistency of parameters: agreement at $O(10^{-5})$ at LO
- At NLO MATRIX, MCFM and FEWZ are in agreement

Validation at LO and NLO

- Consistency of parameters: agreement at $O(10^{-5})$ at LO
- At NLO MATRIX, MCFM and FEWZ are in agreement
- DYNNLO provides predictions
  - accurate typically up to a few per mill and deviate in particular for distributions with challenging kinematics

Validation at LO and NLO

- Consistency of parameters: agreement at $O(10^{-5})$ at LO
- At NLO MATRIX, MCFM and FEWZ are in agreement
- DYNNLO provides predictions
  - accurate typically up to a few per mill and deviate in particular for distributions with challenging kinematics
  - with deviations displaying a particular pattern as a function of the (di-)lepton pseudo-rapidities

see Appendix for details

Comparison of NNLO cross sections
(see Appendix for more details)

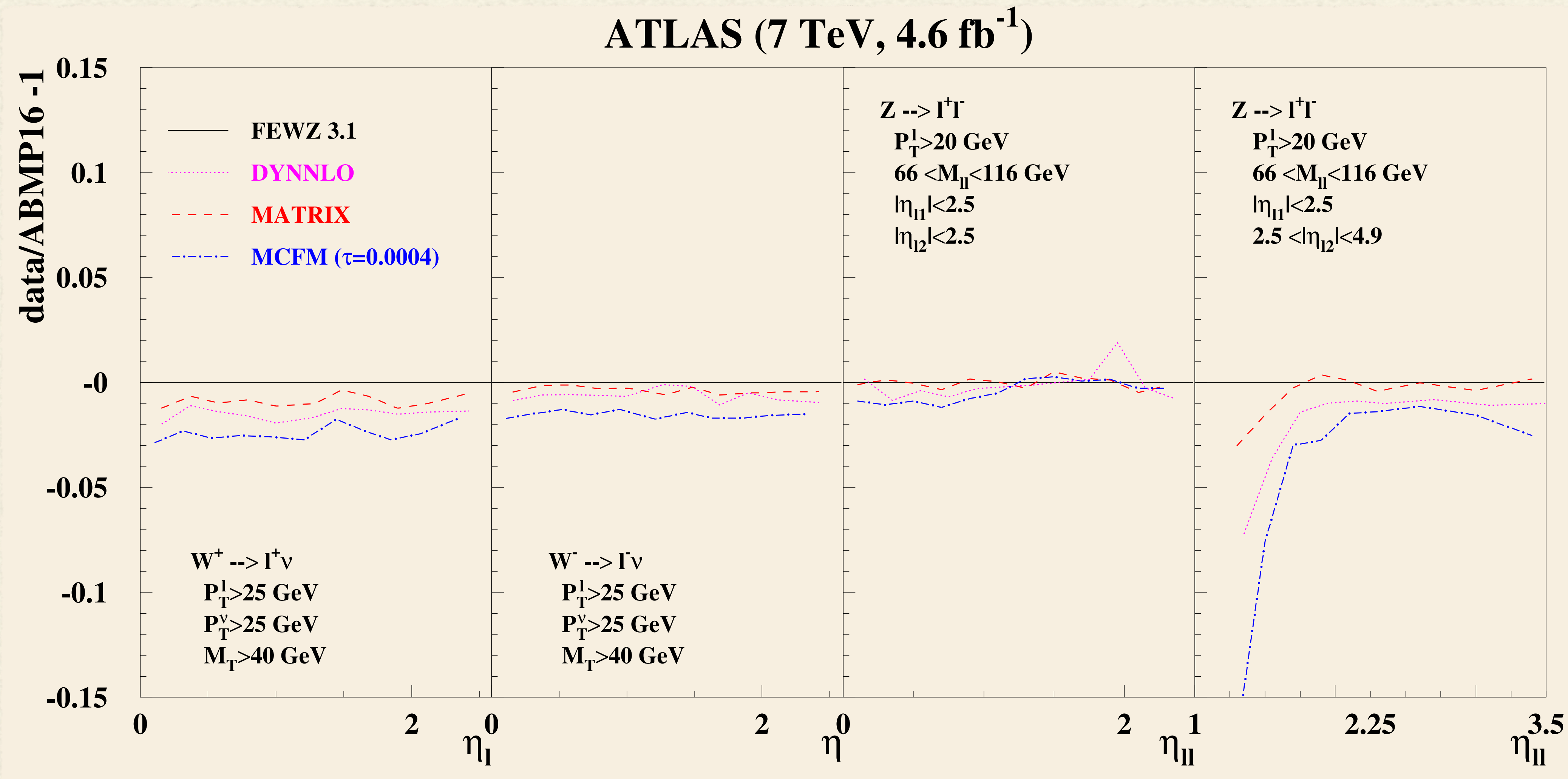

NNLO QCD cross sections for inclusive $pp \to W^\pm + X \to l^\pm \nu + X$ and $pp \to Z/\gamma^* + X \to l^+ l^- + X$ as function of pseudo-rapidity, fiducial cuts are indicated in the plots

$r_{\min} = 0.15(0.05)\%$ for $pp \to W^\pm$ (Z/γ^*) (MATRIX) and $\tau_{\mathrm{cut}} = 4 \cdot 10^{-4}$ (MCFM)

Differences at NNLO

- uncertainties in the cross sections from the numerical Monte Carlo integration have been limited to few units in 10^{-4} and are negligible in all cases

Differences at NNLO

- uncertainties in the cross sections from the numerical Monte Carlo integration have been limited to few units in 10^{-4} and are negligible in all cases
- for most of the distributions considered, the pure NNLO QCD corrections on top of the NLO ones are rather small, often in the range of $\mathrm{O}(1\%)$

Differences at NNLO

- uncertainties in the cross sections from the numerical Monte Carlo integration have been limited to few units in 10^{-4} and are negligible in all cases
- for most of the distributions considered, the pure NNLO QCD corrections on top of the NLO ones are rather small, often in the range of $O(1\%)$
- at NNLO accuracy we found differences among the predictions comparable in size to the NNLO correction itself

Differences at NNLO

- uncertainties in the cross sections from the numerical Monte Carlo integration have been limited to few units in 10^{-4} and are negligible in all cases
- for most of the distributions considered, the pure NNLO QCD corrections on top of the NLO ones are rather small, often in the range of $O(1\%)$
- at NNLO accuracy we found differences among the predictions comparable in size to the NNLO correction itself
- deviations among the predictions are not smaller, often even of the same size or larger, hinting towards a significant intrinsic uncertainty in the computation of the NNLO QCD corrections for those observables

Differences at NNLO

- uncertainties in the cross sections from the numerical Monte Carlo integration have been limited to few units in 10^{-4} and are negligible in all cases
- for most of the distributions considered, the pure NNLO QCD corrections on top of the NLO ones are rather small, often in the range of $O(1\%)$
- at NNLO accuracy we found differences among the predictions comparable in size to the NNLO correction itself
- deviations among the predictions are not smaller, often even of the same size or larger, hinting towards a significant intrinsic uncertainty in the computation of the NNLO QCD corrections for those observables
- the deviations share certain patterns across the range of pseudo-rapidities in the considered distributions

Emergence of the power corrections

- global slicing methods neglect power corrections, hence one may assume that those are at least partly responsible for the observed differences

Emergence of the power corrections

- global slicing methods neglect power corrections, hence one may assume that those are at least partly responsible for the observed differences
- the cross section can be decomposed as

$$\sigma = \int d\tau \frac{d\sigma}{d\tau} = \int^{\tau_{\rm cut}} d\tau \frac{d\sigma}{d\tau} + \int_{\tau_{\rm cut}} d\tau \frac{d\sigma}{d\tau} = \sigma(\tau_{\rm cut}) + \int_{\tau_{\rm cut}} d\tau \frac{d\sigma}{d\tau}$$

Emergence of the power corrections

- global slicing methods neglect power corrections, hence one may assume that those are at least partly responsible for the observed differences
- the cross section can be decomposed as

$$\sigma = \int d\tau \frac{d\sigma}{d\tau} = \int^{\tau_{\rm cut}} d\tau \frac{d\sigma}{d\tau} + \int_{\tau_{\rm cut}} d\tau \frac{d\sigma}{d\tau} = \sigma(\tau_{\rm cut}) + \int_{\tau_{\rm cut}} d\tau \frac{d\sigma}{d\tau}$$

where

$$\frac{d\sigma}{d\tau} \sim \delta(\tau) + \sum_i \left[\frac{\ln^i \tau}{\tau}\right]_+ + \sum_j \tau^{p-1} \ln^j \tau + \mathcal{O}(\tau^p)$$

from universal soft and collinear QCD factorization

Emergence of the power corrections

- global slicing methods neglect power corrections, hence one may assume that those are at least partly responsible for the observed differences
- the cross section can be decomposed as

$$\sigma = \int d\tau \frac{d\sigma}{d\tau} = \int^{\tau_{\mathrm{cut}}} d\tau \frac{d\sigma}{d\tau} + \int_{\tau_{\mathrm{cut}}} d\tau \frac{d\sigma}{d\tau} = \sigma(\tau_{\mathrm{cut}}) + \int_{\tau_{\mathrm{cut}}} d\tau \frac{d\sigma}{d\tau}$$

where

$$\frac{d\sigma}{d\tau} \sim \delta(\tau) + \sum_i \left[\frac{\ln^i \tau}{\tau}\right]_+ + \sum_j \tau^{p-1} \ln^j \tau + \mathcal{O}(\tau^p)$$

from universal soft and collinear QCD factorization

- hence (schematically)

$$\sigma(\tau_{\mathrm{cut}}) \sim 1 + \sum_i \ln^{i+1} \tau_{\mathrm{cut}} + \sum_j \tau_{\mathrm{cut}}^p \ln^j \tau_{\mathrm{cut}} + \mathcal{O}(\tau_{\mathrm{cut}}^{p+1})$$

Power corrections and fiducial cuts

- the power p takes
  - positive integer values for the production of a stable gauge boson V

Power corrections and fiducial cuts

- the power p takes
  - positive integer values for the production of a stable gauge boson V
  - half-integers, i.e., $p = 1/2,\ 1,\ 3/2$ for subsequent decay with cuts on the leptonic final state

Power corrections and fiducial cuts

- the power p takes
  - positive integer values for the production of a stable gauge boson V
  - half-integers, i.e., $p = 1/2,\ 1,\ 3/2$ for subsequent decay with cuts on the leptonic final state
- the global subtraction schemes are implemented via a global subtraction term $\sigma^{\mathrm{sub}}(\tau_{\mathrm{cut}})$ as

$$\sigma \;=\; \sigma^{\mathrm{sub}}(\tau_{\mathrm{cut}}) + \int_{\tau_{\mathrm{cut}}} d\tau \, \frac{d\sigma}{d\tau} + \Delta\sigma^{\mathrm{sub}}(\tau_{\mathrm{cut}})$$

Power corrections and fiducial cuts

- the power p takes
  - positive integer values for the production of a stable gauge boson V
  - half-integers, i.e., $p = 1/2,\ 1,\ 3/2$ for subsequent decay with cuts on the leptonic final state

- the global subtraction schemes are implemented via a global subtraction term $\sigma^{\rm sub}(\tau_{\rm cut})$ as

$$\sigma \;=\; \sigma^{\rm sub}(\tau_{\rm cut}) + \int_{\tau_{\rm cut}} d\tau \, \frac{d\sigma}{d\tau} + \cancel{\Delta\sigma^{\rm sub}(\tau_{\rm cut})}$$

where $\Delta\sigma^{\rm sub}(\tau_{\rm cut}) = \sigma(\tau_{\rm cut}) - \sigma^{\rm sub}(\tau_{\rm cut})$ parametrizes the residual power corrections that are neglected in slicing methods, resulting in an intrinsic error

Power corrections and fiducial cuts

- the power p takes
  - positive integer values for the production of a stable gauge boson V
  - half-integers, i.e., $p = 1/2,\ 1,\ 3/2$ for subsequent decay with cuts on the leptonic final state
- the global subtraction schemes are implemented via a global subtraction term $\sigma^{\text{sub}}(\tau_{\text{cut}})$ as

$$\sigma \;=\; \sigma^{\text{sub}}(\tau_{\text{cut}}) + \int_{\tau_{\text{cut}}} d\tau\, \frac{d\sigma}{d\tau} + \cancel{\Delta\sigma^{\text{sub}}(\tau_{\text{cut}})}$$

where $\Delta\sigma^{\text{sub}}(\tau_{\text{cut}}) = \sigma(\tau_{\text{cut}}) - \sigma^{\text{sub}}(\tau_{\text{cut}})$ parametrizes the residual power corrections that are neglected in slicing methods, resulting in an intrinsic error

- If the global subtraction term cancels only the leading soft and collinear singularities in σ then the residual power corrections in the presence of cuts on the decay leptons are enhanced to linear in q_T

Lepton phase space and fiducial cuts

- the lepton phase space is ($q = p_1 + p_2$)

$$\Phi_L(q_T) = \left(\int \prod_{i=1}^{2} \frac{d^4 p_i}{(2\pi)^3} \delta^+(p_i^2) \right) (2\pi)^4 \delta^{(4)}(q - p_1 - p_2) = \frac{1}{4\pi^2} \int_0^{\pi} d\phi \int_{-\infty}^{\infty} d\Delta y \, \frac{p_{T1}^2}{Q^2}$$

Lepton phase space and fiducial cuts

- the lepton phase space is ($q = p_1 + p_2$)

$$\Phi_L(q_T) = \left(\int \prod_{i=1}^{2} \frac{d^4 p_i}{(2\pi)^3} \delta^+(p_i^2) \right) (2\pi)^4 \delta^{(4)}(q - p_1 - p_2) = \frac{1}{4\pi^2} \int_0^\pi d\phi \int_{-\infty}^{\infty} d\Delta y \, \frac{p_{T1}^2}{Q^2}$$

- after employing typical fiducial cuts, it reads as

$$\Phi_L(q_T) = \frac{1}{4\pi^2} \int_0^\pi d\phi \int_{-\infty}^{\infty} d\Delta y \, \frac{p_{T1}^2}{Q^2} \left(\prod_{i=1}^{2} \theta(p_{Ti} - p_T^{\min}) \theta(\eta_i - \eta_i^{\min}) \theta(\eta_i^{\max} - \eta_i) \right)$$

Lepton phase space and fiducial cuts

- the lepton phase space is ($q = p_1 + p_2$)

$$\Phi_L(q_T) = \left(\int \prod_{i=1}^{2} \frac{d^4 p_i}{(2\pi)^3} \delta^+(p_i^2) \right) (2\pi)^4 \delta^{(4)}(q - p_1 - p_2) = \frac{1}{4\pi^2} \int_0^{\pi} d\phi \int_{-\infty}^{\infty} d\Delta y \, \frac{p_{T1}^2}{Q^2}$$

- after employing typical fiducial cuts, it reads as

$$\Phi_L(q_T) = \frac{1}{4\pi^2} \int_0^{\pi} d\phi \int_{-\infty}^{\infty} d\Delta y \, \frac{p_{T1}^2}{Q^2} \left(\prod_{i=1}^{2} \theta(p_{Ti} - p_T^{\min}) \theta(\eta_i - \eta_i^{\min}) \theta(\eta_i^{\max} - \eta_i) \right)$$

- the θ-functions break azimuthal symmetry in some parts of the phase space due to rapidity cuts — leading to linear power corrections —, whose boundary is given by q_T^* obtained as

$$\frac{q_T^*}{Q} = \frac{|Y|}{\sinh(\eta^{\max})} + \mathcal{O}(Y)$$

Lepton phase space and fiducial cuts

- the lepton phase space is ($q = p_1 + p_2$)

$$\Phi_L(q_T) = \left(\int \prod_{i=1}^{2} \frac{d^4 p_i}{(2\pi)^3} \delta^+(p_i^2) \right) (2\pi)^4 \delta^{(4)}(q - p_1 - p_2) = \frac{1}{4\pi^2} \int_0^\pi d\phi \int_{-\infty}^{\infty} d\Delta y \, \frac{p_{T1}^2}{Q^2}$$

- after employing typical fiducial cuts, it reads as

$$\Phi_L(q_T) = \frac{1}{4\pi^2} \int_0^\pi d\phi \int_{-\infty}^{\infty} d\Delta y \, \frac{p_{T1}^2}{Q^2} \left(\prod_{i=1}^{2} \theta(p_{Ti} - p_T^{\min}) \theta(\eta_i - \eta_i^{\min}) \theta(\eta_i^{\max} - \eta_i) \right)$$

- the θ-functions break azimuthal symmetry in some parts of the phase space due to rapidity cuts — leading to linear power corrections —, whose boundary is given by q_T^* obtained as

$$\frac{q_T^*}{Q} = \frac{|Y|}{\sinh(\eta^{\max})} + \mathcal{O}(Y)$$

with Y being the pseudo rapidity of the gauge boson

Lepton phase space and fiducial cuts

- the lepton phase space is ($q = p_1 + p_2$)

$$\Phi_L(q_T) = \left(\int \prod_{i=1}^{2} \frac{d^4 p_i}{(2\pi)^3}\, \delta^+(p_i^2)\right)(2\pi)^4\, \delta^{(4)}(q - p_1 - p_2) = \frac{1}{4\pi^2}\int_0^{\pi} d\phi \int_{-\infty}^{\infty} d\Delta y\, \frac{p_{T1}^2}{Q^2}$$

- after employing typical fiducial cuts, it reads as

$$\Phi_L(q_T) = \frac{1}{4\pi^2}\int_0^{\pi} d\phi \int_{-\infty}^{\infty} d\Delta y\, \frac{p_{T1}^2}{Q^2}\left(\prod_{i=1}^{2} \theta(p_{Ti} - p_T^{\min})\,\theta(\eta_i - \eta_i^{\min})\theta(\eta_i^{\max} - \eta_i)\right)$$

- the θ-functions break azimuthal symmetry in some parts of the phase space due to rapidity cuts — leading to linear power corrections —, whose boundary is given by $q_T{}^*$ obtained as

$$\frac{q_T^*}{Q} = \frac{|Y|}{\sinh(\eta^{\max})} + \mathcal{O}(Y)$$

with Y being the pseudo rapidity of the gauge boson

- for $q_T < q_T{}^*$ azimuthal symmetry is restored, and power corrections are quadratic

Lepton phase space and fiducial cuts

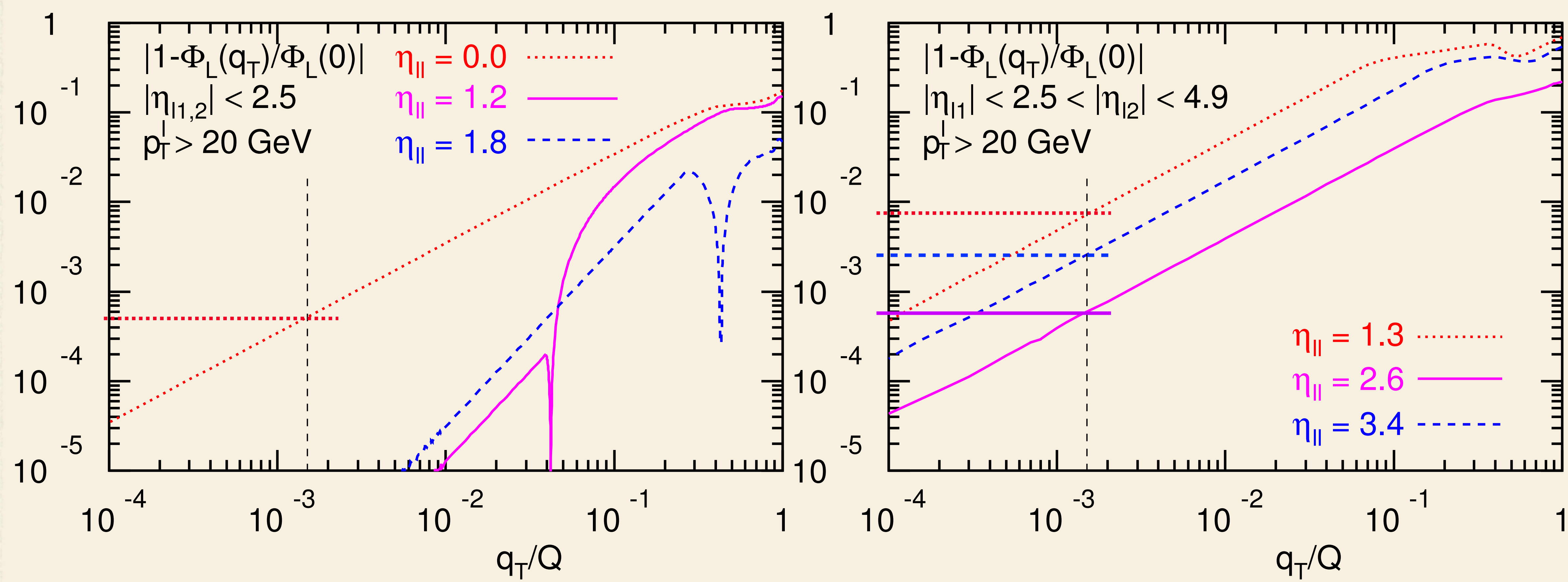

difference between the Born and real emission phase spaces $\Phi_L(0) - \Phi_L(q_T)$ of the decay leptons relative to the Born one at fiducial cuts applied to ATLAS data set for Z/γ^*-boson production ($Q = M_Z$) for different values of the gauge boson pseudo-rapidity η_{ll}, $p^l_T \geq 20$ GeV. Left: cuts selecting central pseudo-rapidities. Right: Cuts selecting one lepton at central pseudo-rapidity and the other at forward pseudo-rapidity. The vertical dashed line indicates the minimum value $r_{\rm cut} = 0.15\%$ used in **MATRIX** as a slicing cut

Recall: MATRIX vs FEWZ

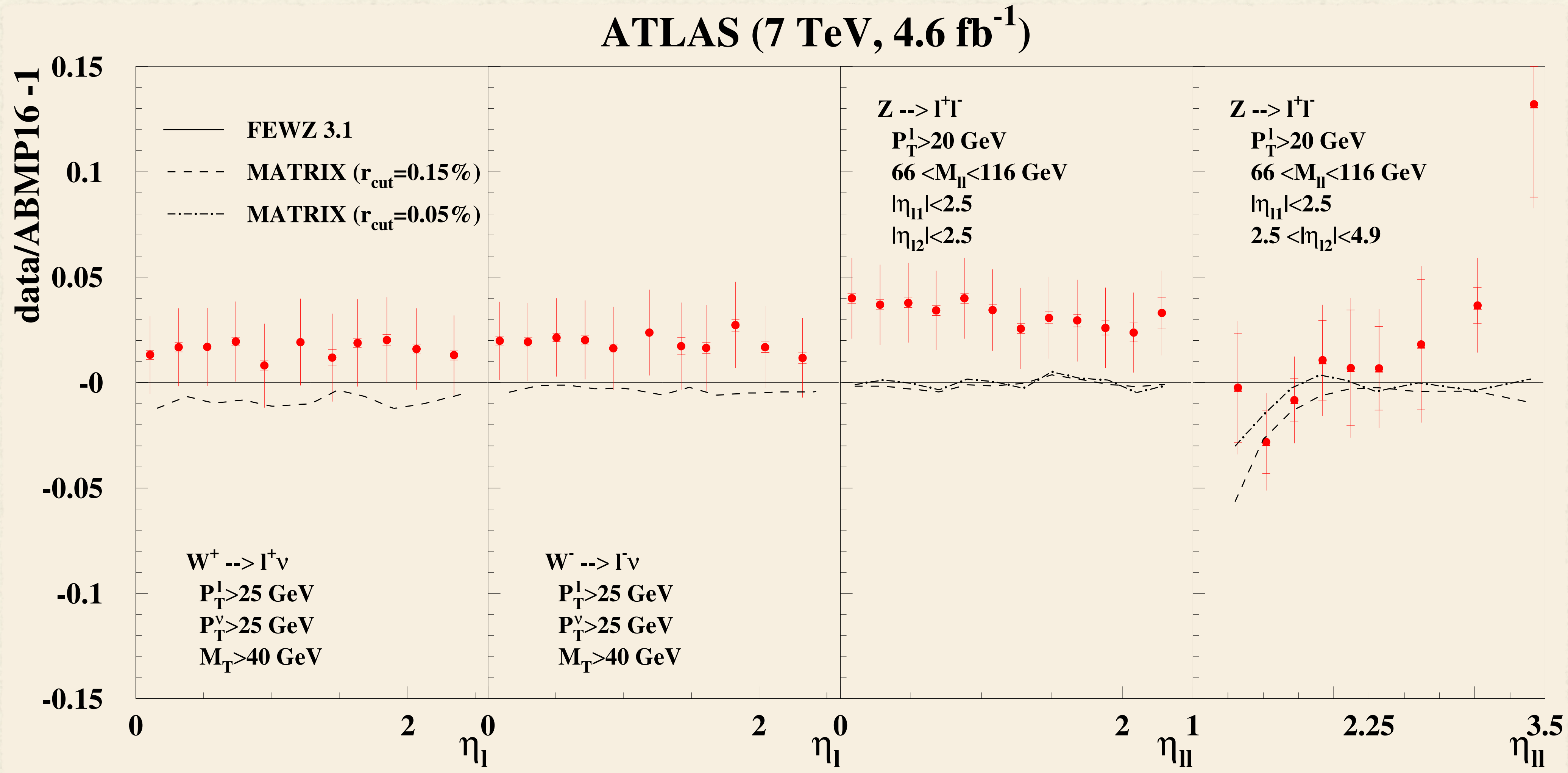

NNLO QCD cross sections for inclusive

$pp \to W^{\pm} + X \to l^{\pm}\nu + X$ and $pp \to Z/\gamma^* + X \to l^+ l^- + X$ as function of pseudo-rapidity,

fiducial cuts as before and indicated in the plots

$r_{cut} = 0.15\%$ (dashed) and $r_{cut} = 0.05\%$ (dashed-dotted)

Conclusions

- ✓ at NLO MATRIX, MCFM and FEWZ are in agreement
- ✓ at NNLO accuracy we found differences among the predictions comparable in size to the NNLO correction itself — see Appendix
- ✓ fiducial cuts on the transverse momenta and pseudo-rapidities of the decay leptons lead to linear power corrections in the slicing parameter
- ✓ deviations share certain patterns across the range of pseudo-rapidities in the considered distributions, which have been correlated with the appearance of linear power corrections in the lepton decay phase space Φ_L as a function of q_T
- ✓ the continuous increase in the precision of the experimental measurements, the theory predictions are pressed to provide cross sections at NNLO (or beyond) where the systematic uncertainties due to choices of particular schemes or algorithms for the computation can be safely neglected in comparison to the experimental uncertainties

Appendix

Validation at NLO

Validation at LO and NLO

- Consistency of parameters: agreement at $\mathrm{O}(10^{-5})$ at LO
- At NLO all but DYNNLO employ local subtraction

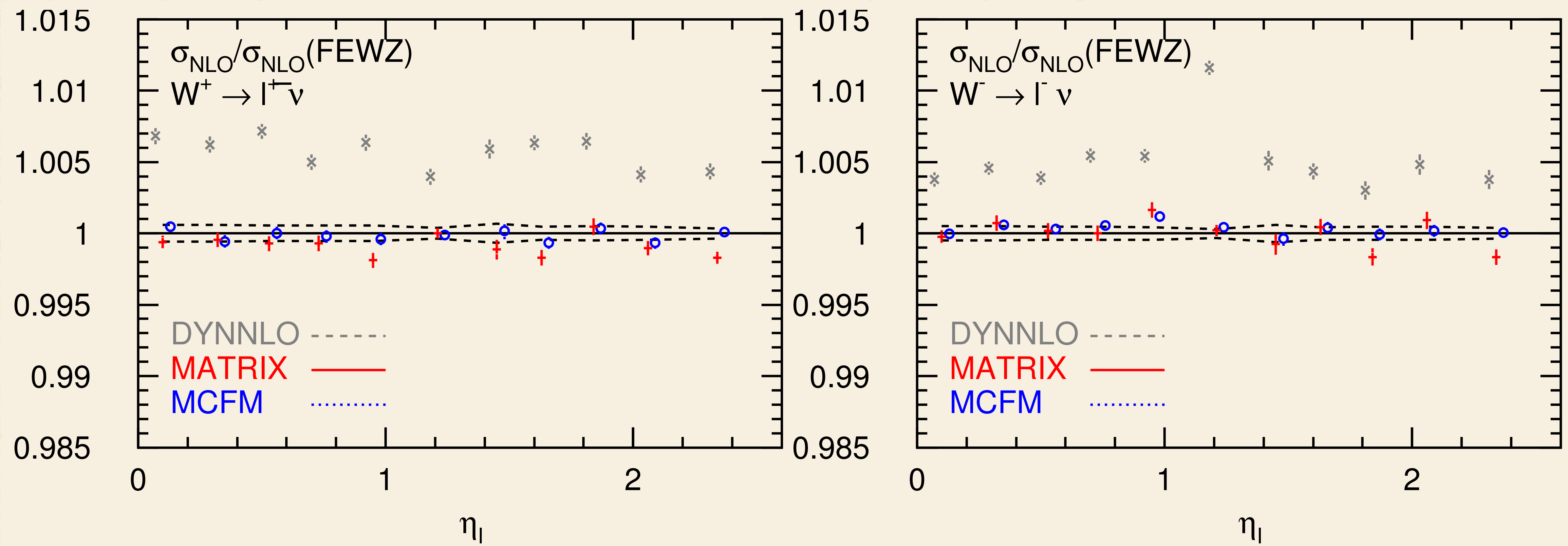

NLO QCD cross sections for inclusive $pp \to W^\pm + X \to l^\pm \nu + X$ as function of pseudo-rapidity, $p^l{}_T, p^\nu{}_T \geq 25$ GeV and $M_T \geq 40$ GeV

Validation at LO and NLO

- At NLO all but DYNNLO employ local subtraction

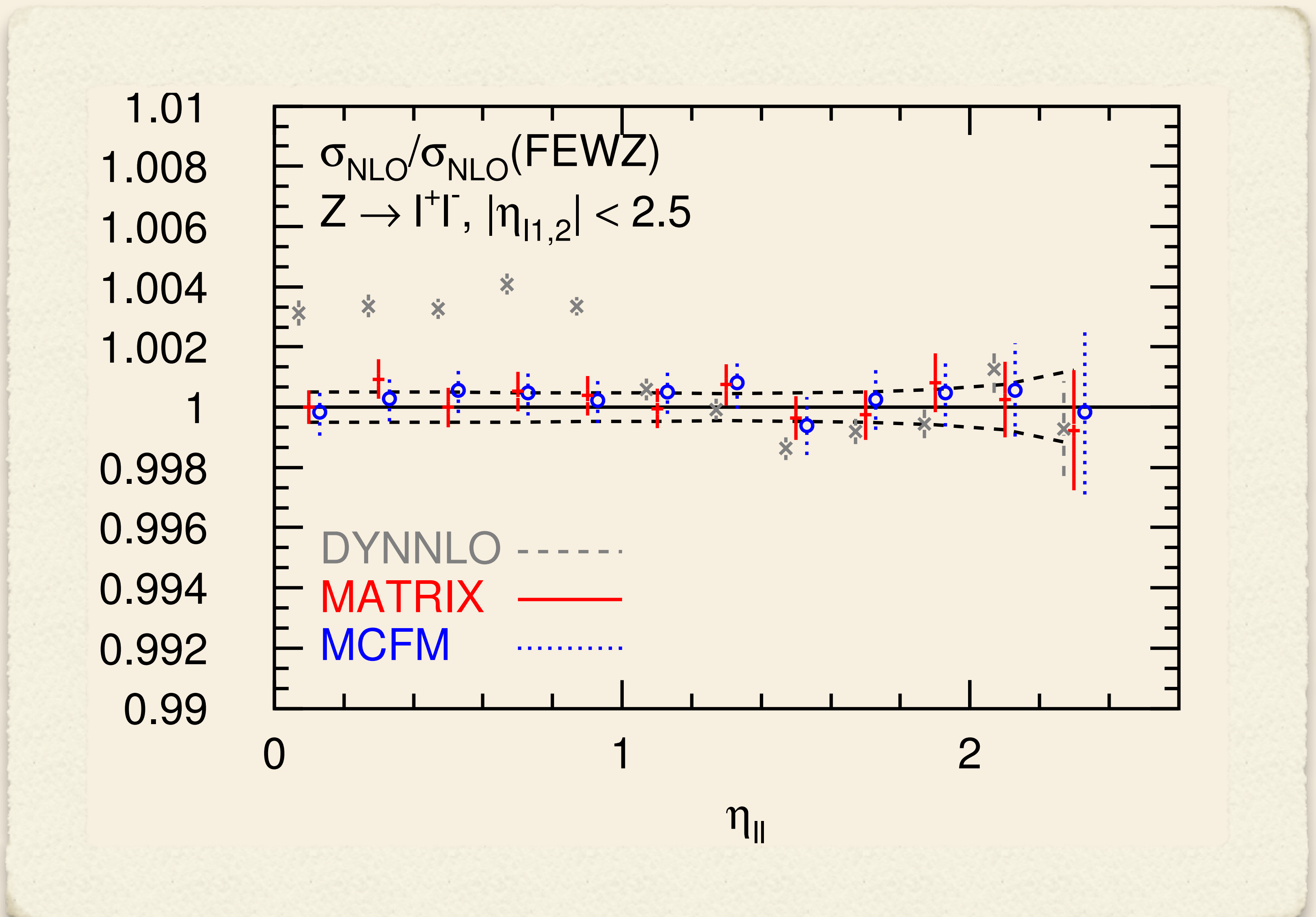

As previous for $pp \to Z/\gamma^* + X \to l^+ l^- + X$, $p^i_T \geq 25$ GeV, $116 \geq M_{ll}/\mathrm{GeV} \geq 66$, $|\eta_{l_i}| \leq 2.5$, $i = 1, 2$

Validation at LO and NLO

- At NLO all but DYNNLO employ local subtraction

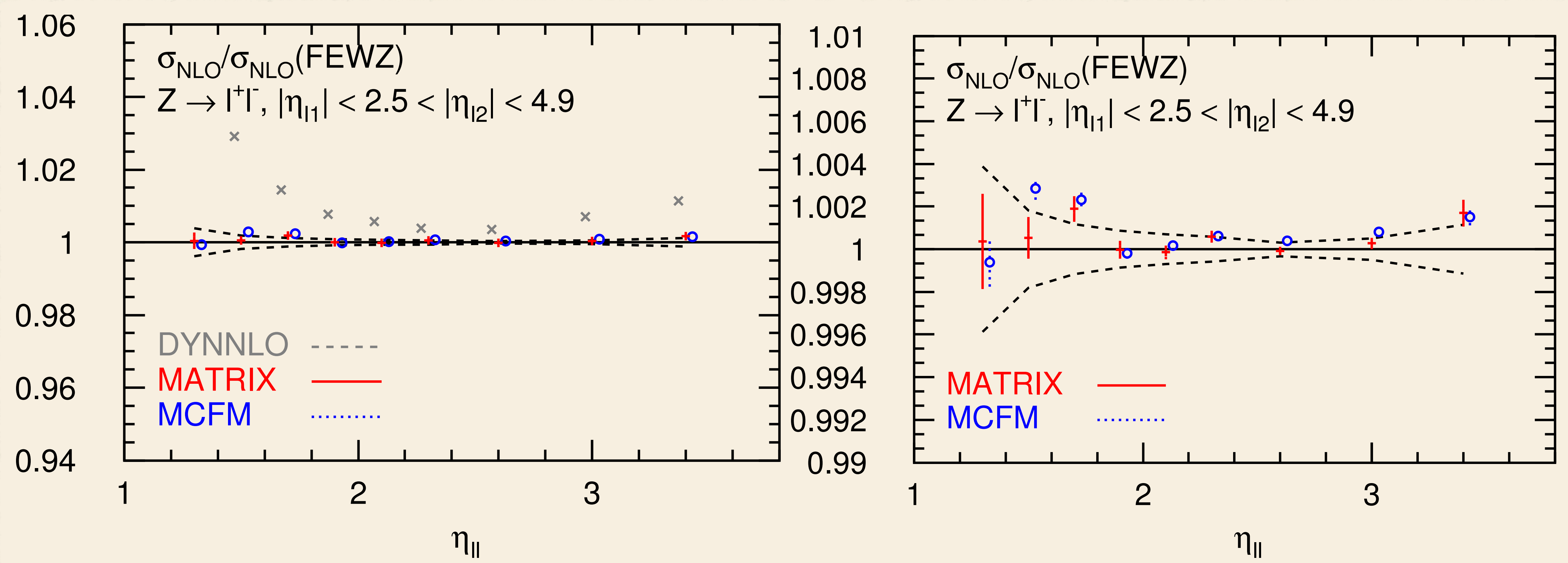

As previous but with $|\eta_{l1}| \leq 2.5,\ 2.5 \leq |\eta_{l2}| \leq 4.9$

Validation at LO and NLO

- Consistency of parameters: agreement at $O(10^{-5})$ at LO
- At NLO all but DYNNLO employ local subtraction

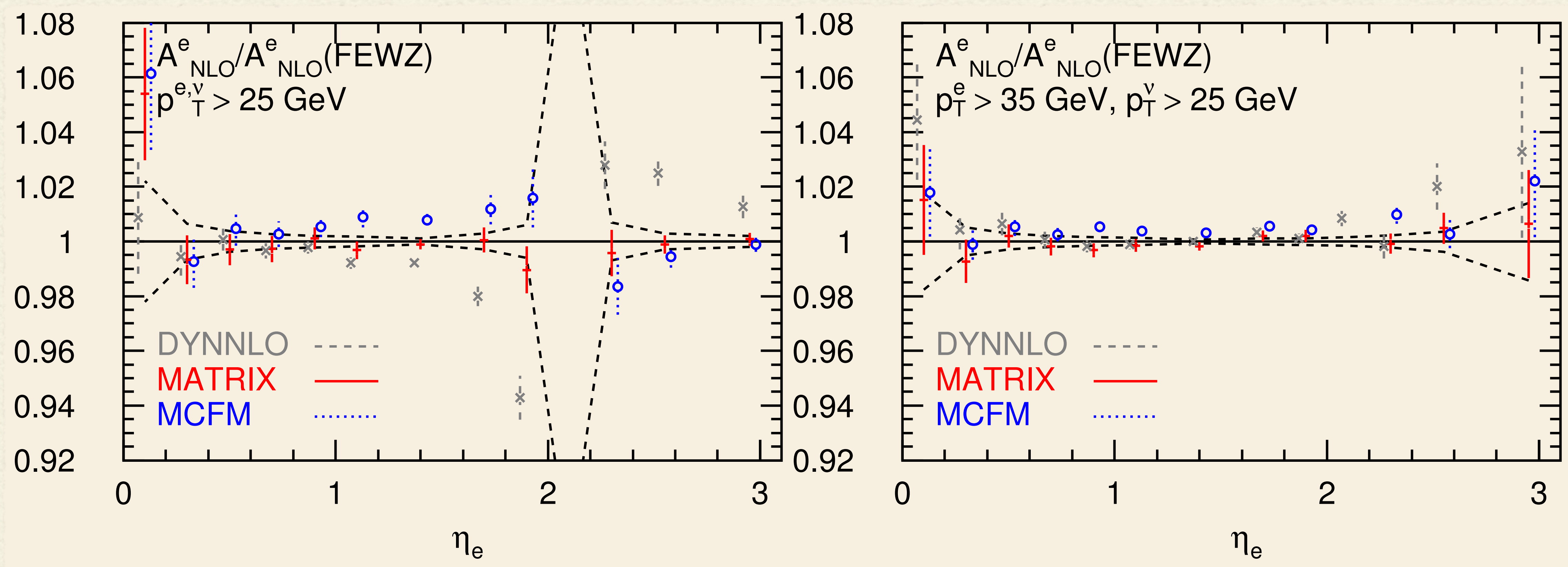

electron charge asymmetry distribution A_e in $W^\pm$ boson production

Left: symmetric cuts, $p^l{}_T, p^\nu{}_T \geq 25$ GeV

Right: staggered cuts $p^l{}_T \geq 35$ GeV, $p^\nu{}_T \geq 25$ GeV

Comparison at NNLO

DYNNLO vs FEWZ

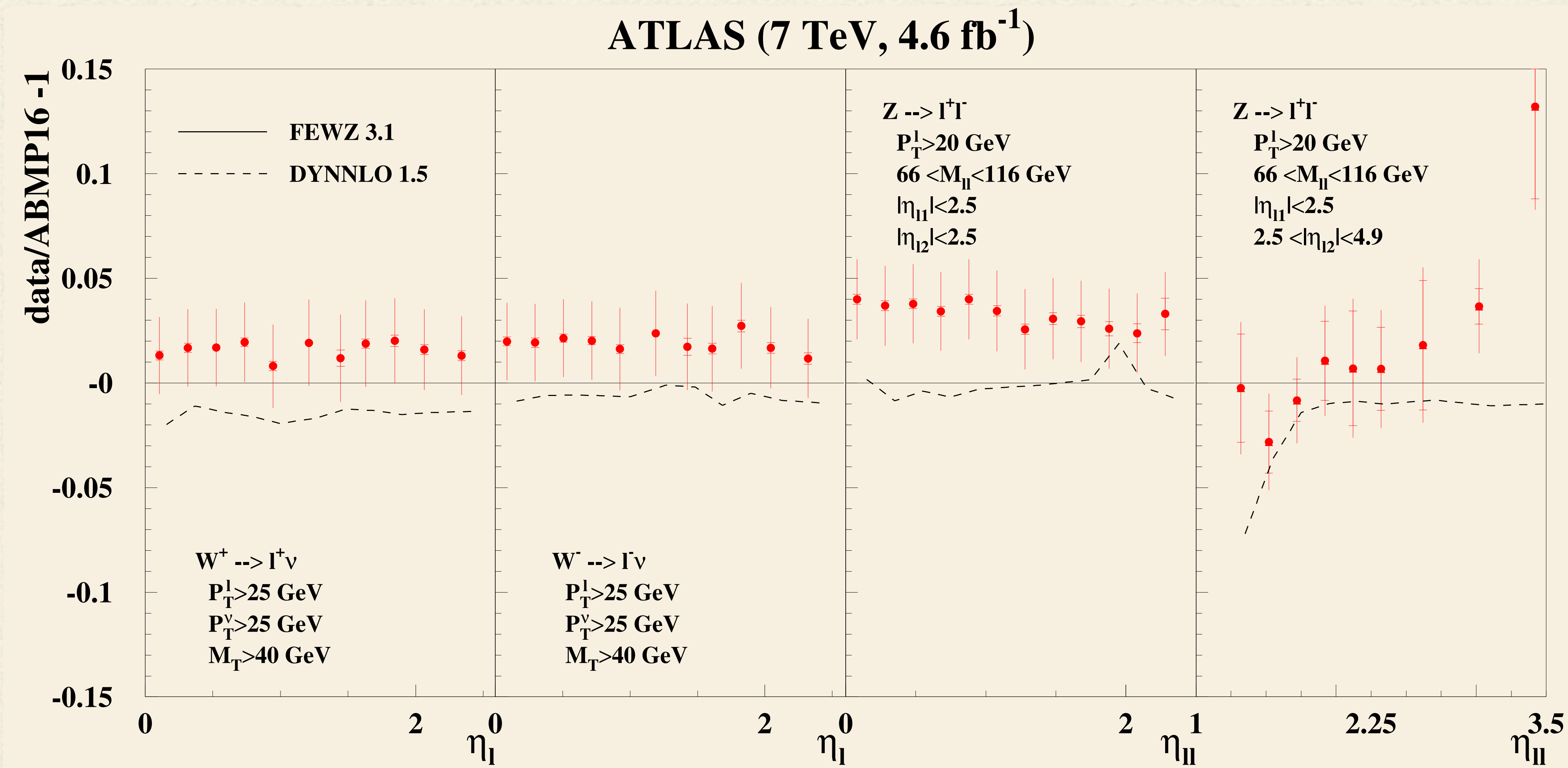

NNLO QCD cross sections for inclusive $pp \to W^{\pm}+X \to l^{\pm}\nu+X$ and $pp \to Z/\gamma^*+X \to l^+l^-+X$ as function of pseudo-rapidity, fiducial cuts as before and indicated in the plots

MATRIX vs FEWZ

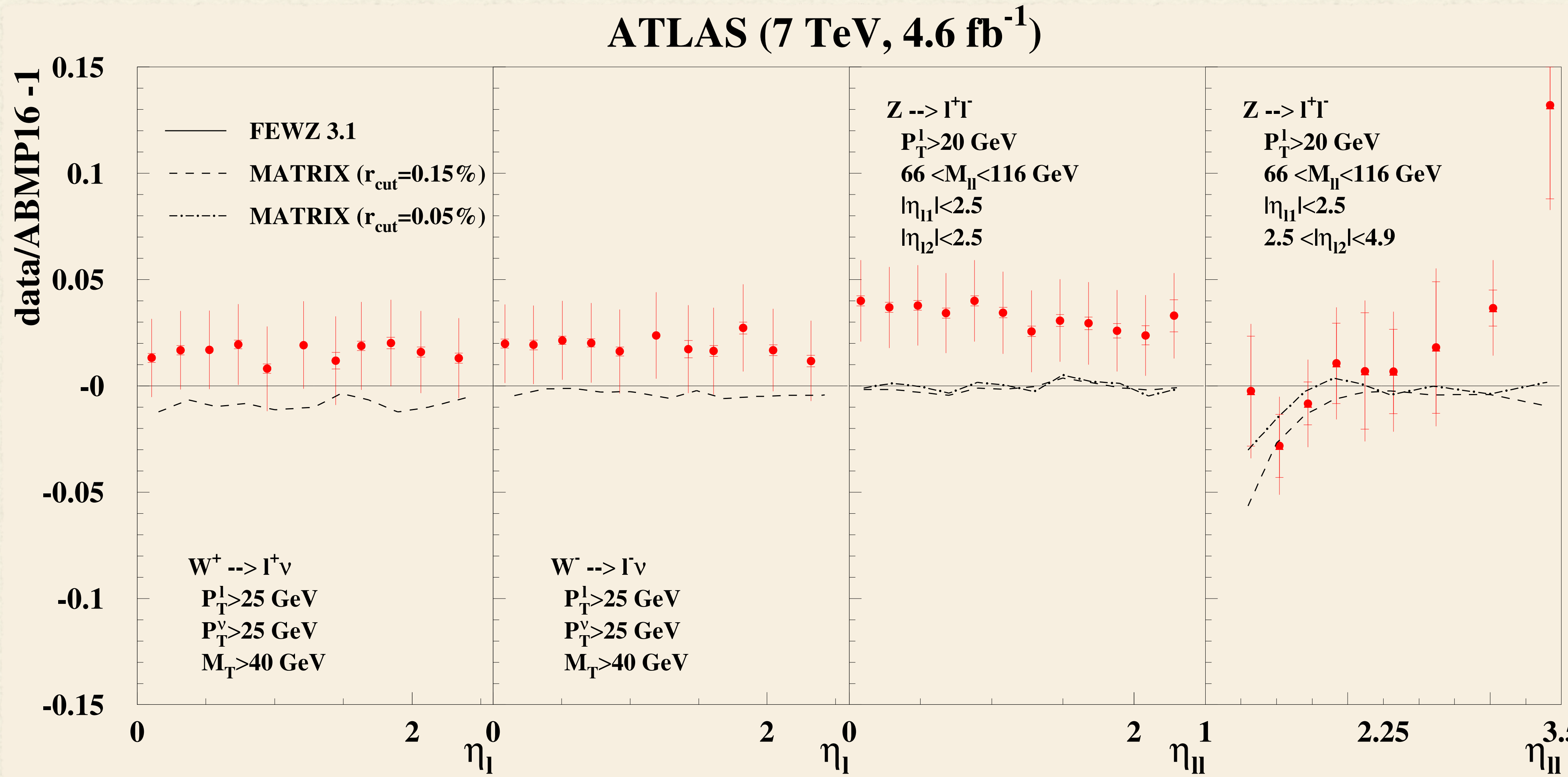

As previous with different values for the q_T-slicing cut:
$r_{\rm cut} = 0.15\%$ (dashed) and $r_{\rm cut} = 0.05\%$ (dashed-dotted)

MCFM vs FEWZ

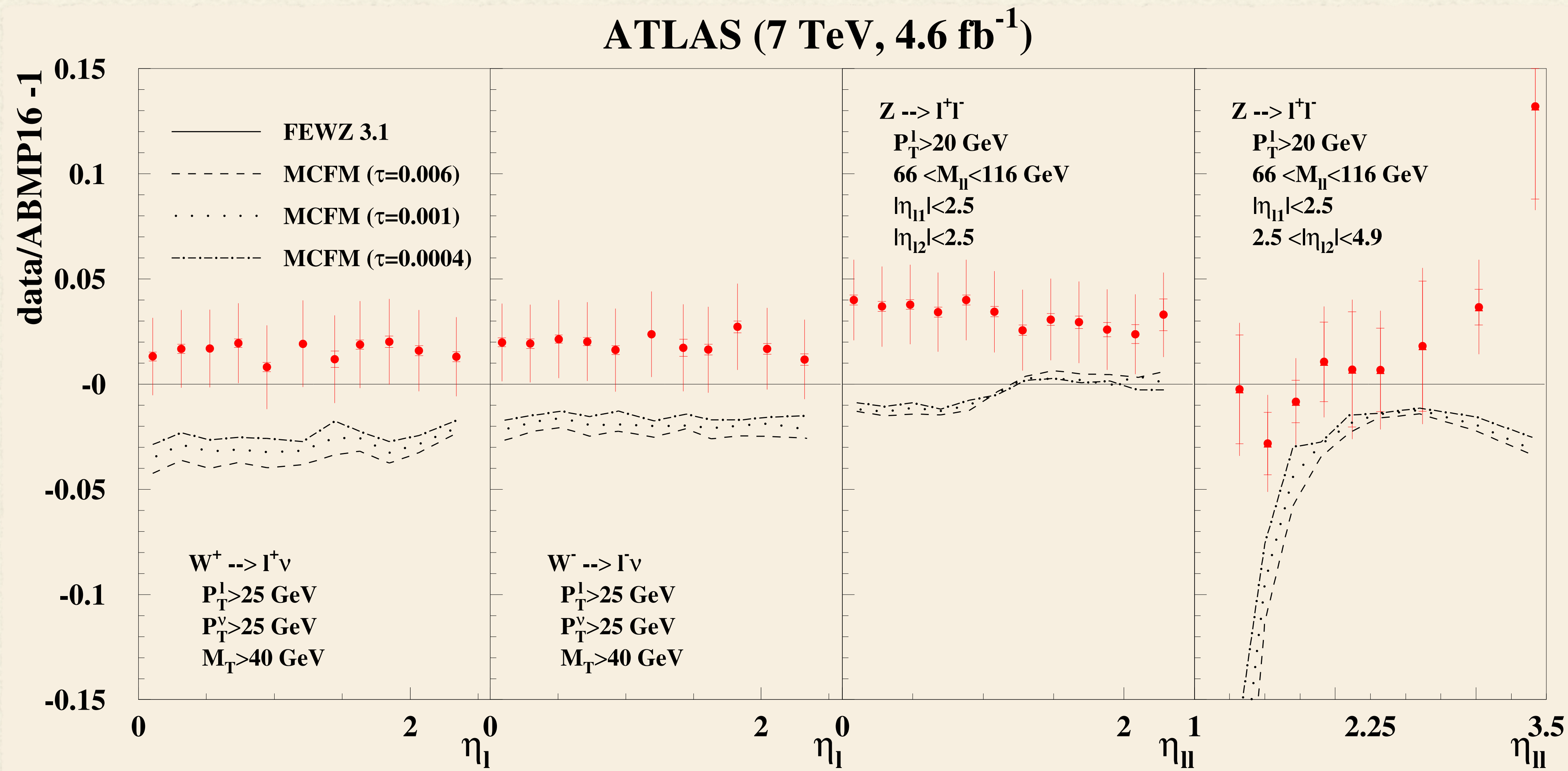

As previous with different values for the jettiness slicing cut:

$\tau_{\rm cut} = 6 \cdot 10^{-3}$ (dashed), $\tau_{\rm cut} = 10^{-3}$ (dotted), $\tau_{\rm cut} = 4 \cdot 10^{-4}$ (dashed-dotted)

DYNNLO vs FEWZ

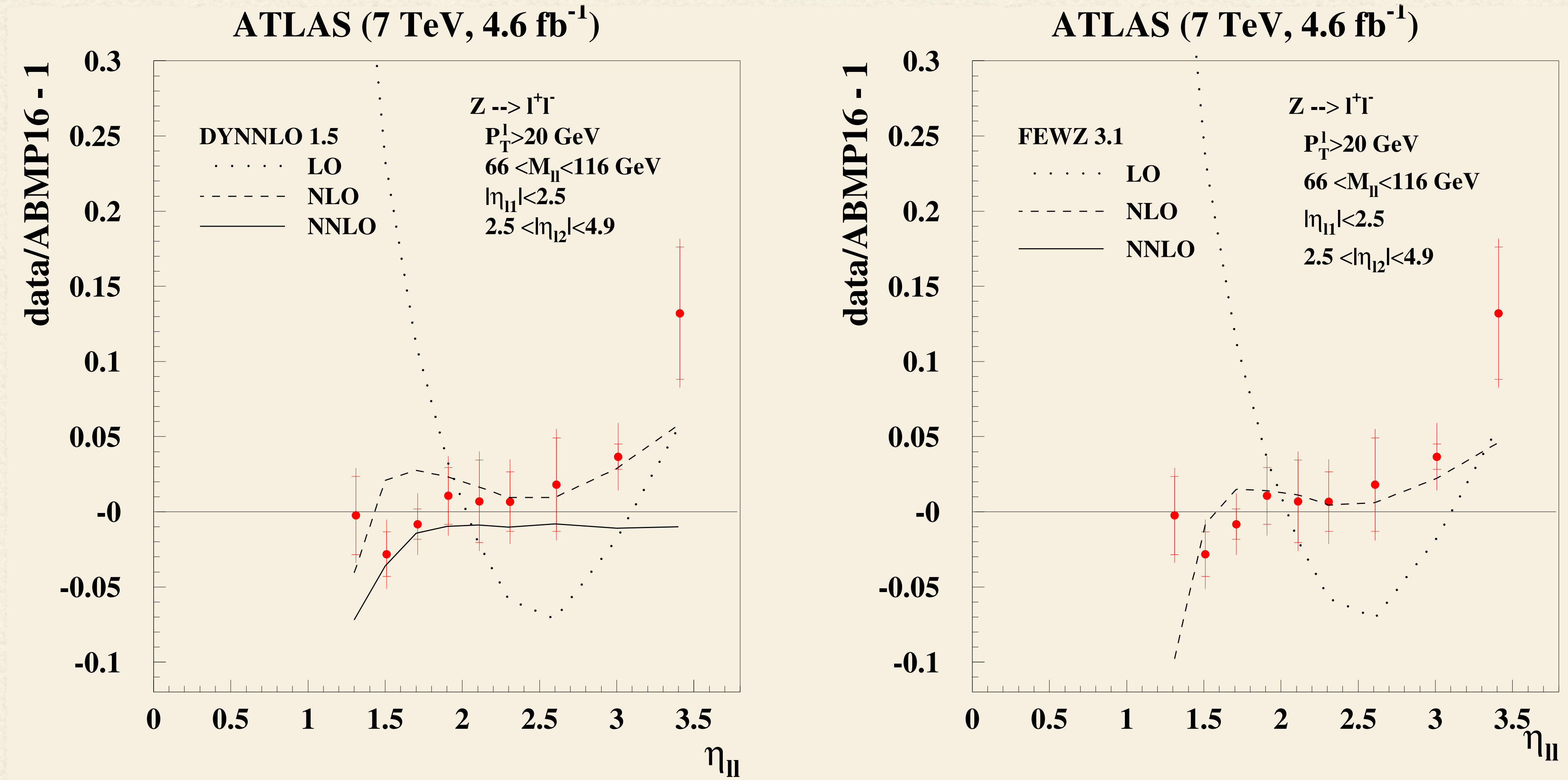

LO, NLO and NNLO QCD cross sections normalized to **FEWZ** at NNLO for inclusive $pp \to Z/\gamma^* + X \to l^+ l^- + X$ as function of pseudo-rapidity of the lepton pair with staggered cuts indicated in the plots

MATRIX and MCFM vs FEWZ

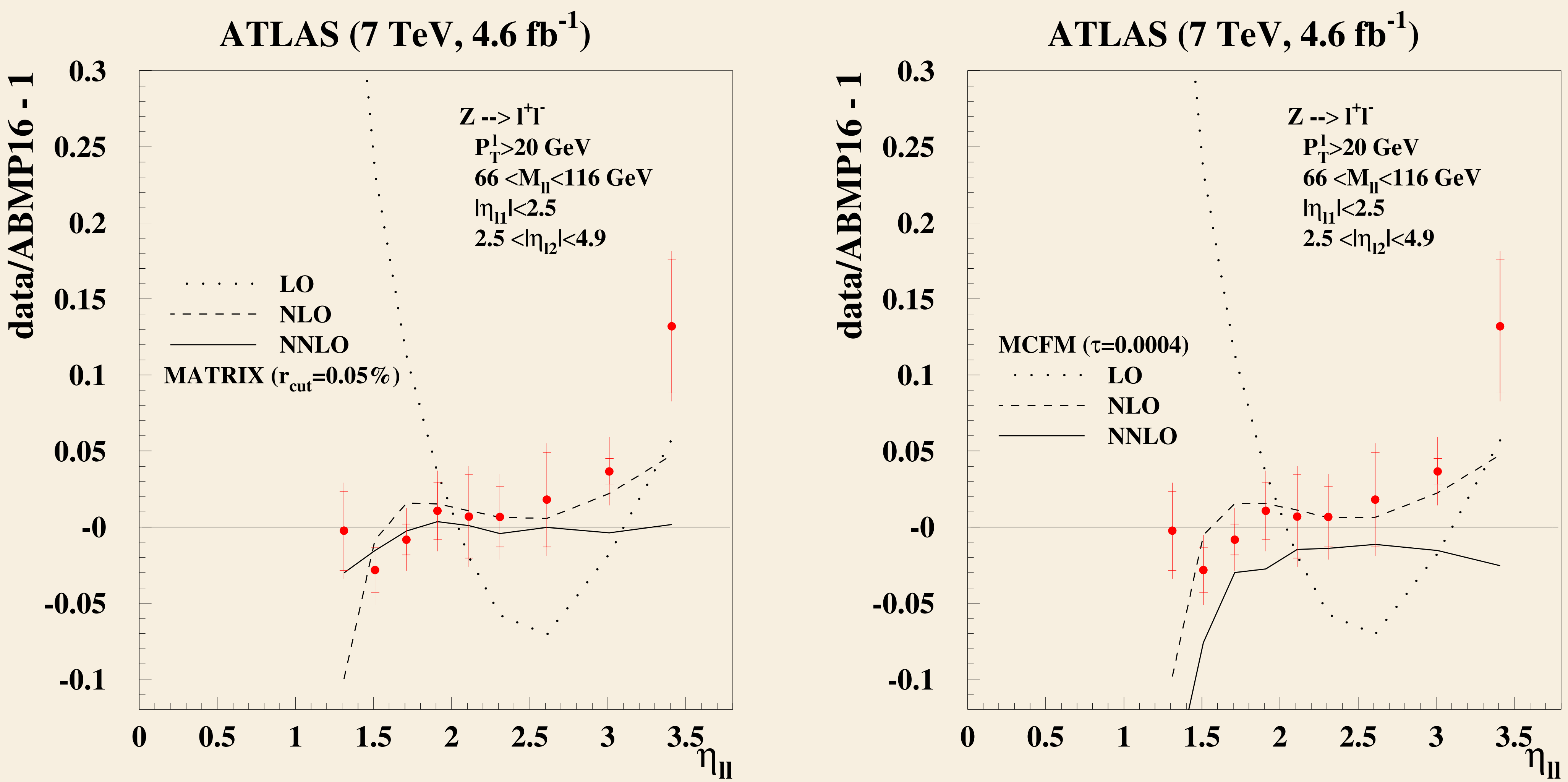

As previous for **MATRIX** (left) and **MCFM** (right)

DYNNLO vs FEWZ

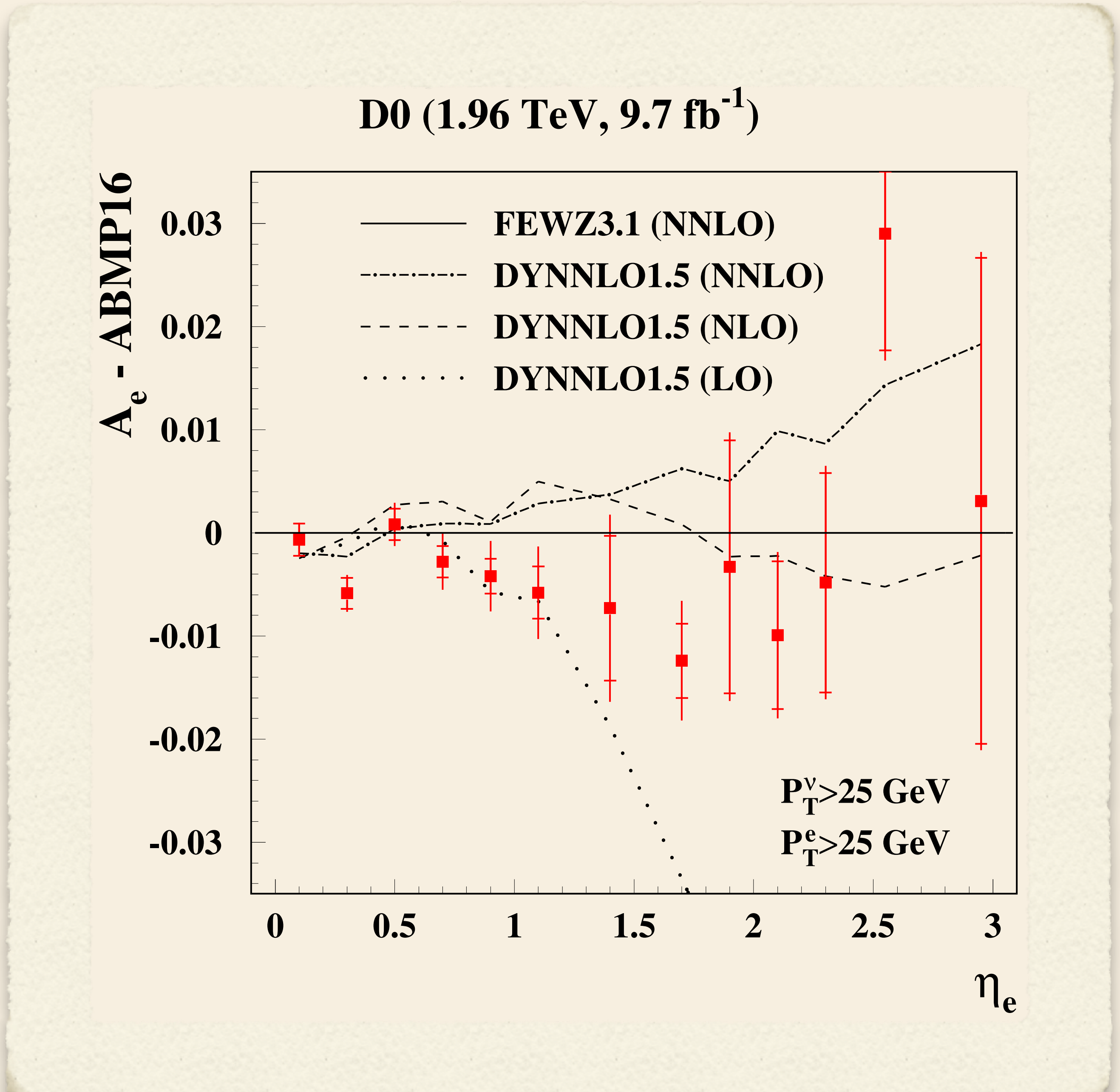

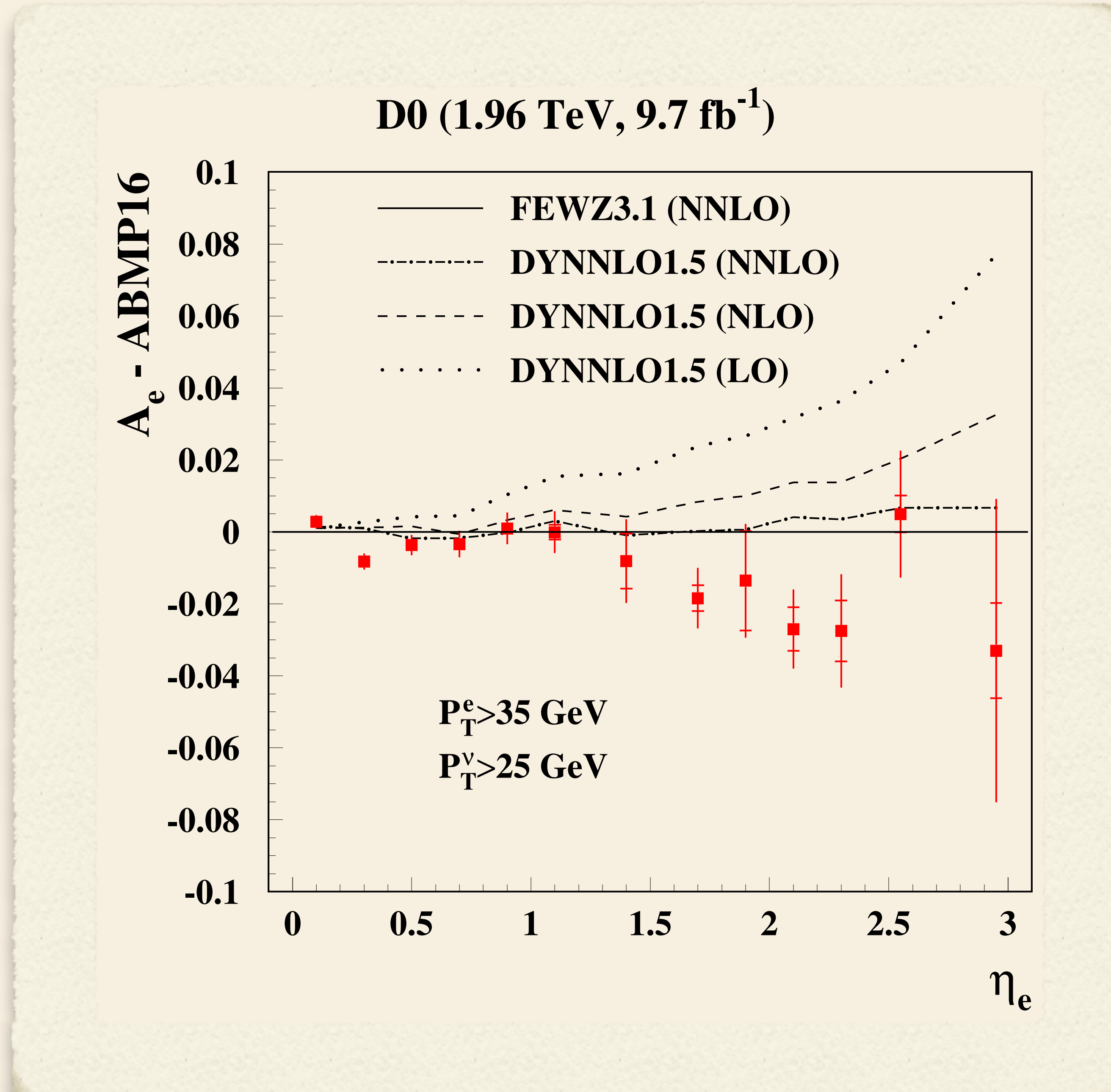

electron charge asymmetry distribution A_e in $W^\pm$ boson production at LO, NLO and NNLO normalized to **FEWZ** at NNLO

Left: symmetric cuts Right: staggered cuts as indicated in the plots

MATRIX vs FEWZ

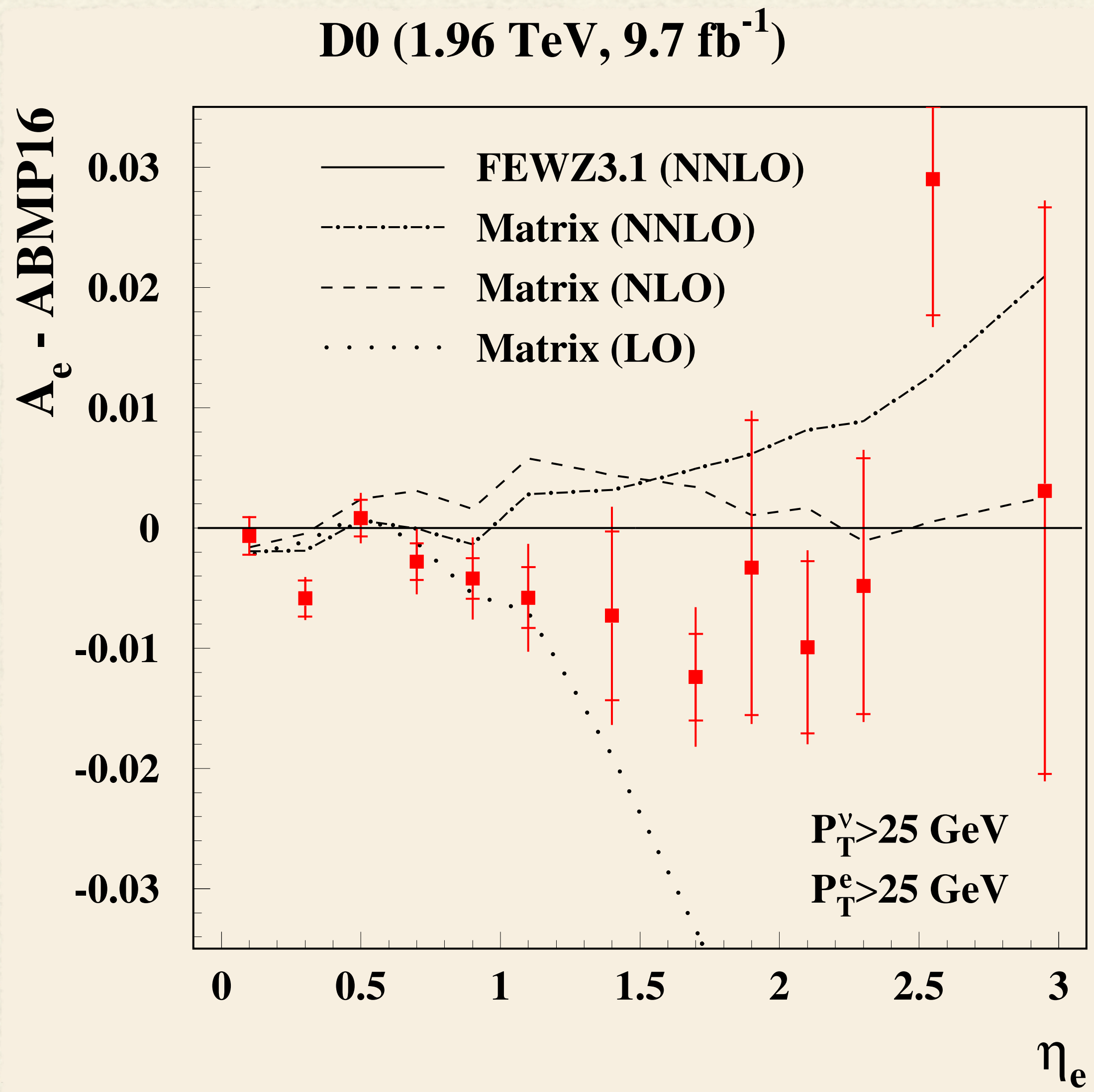

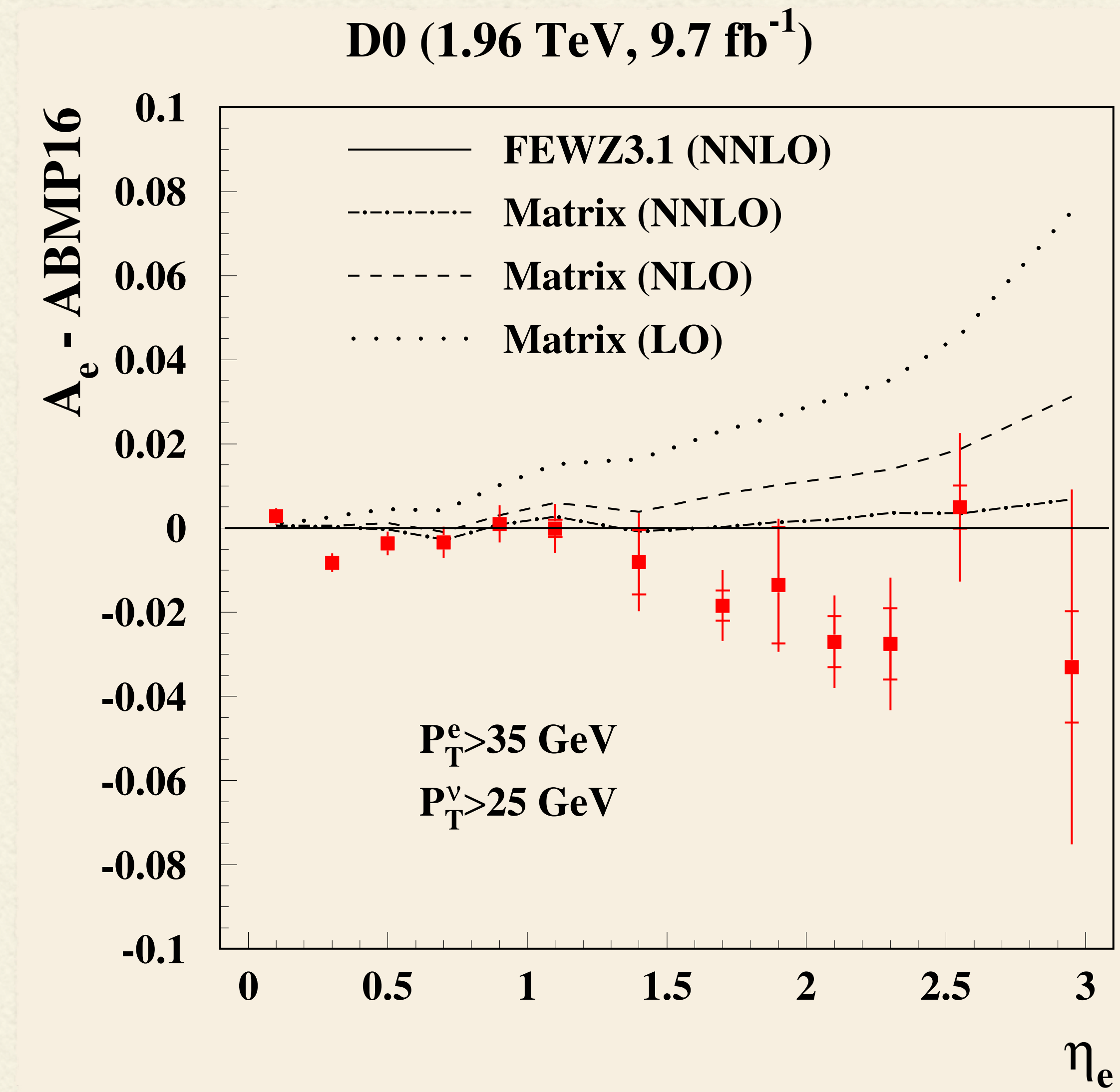

electron charge asymmetry distribution A_e in $W^\pm$ boson production at LO, NLO and NNLO normalized to FEWZ at NNLO

Left: symmetric cuts Right: staggered cuts as indicated in the plots

MCFM vs FEWZ

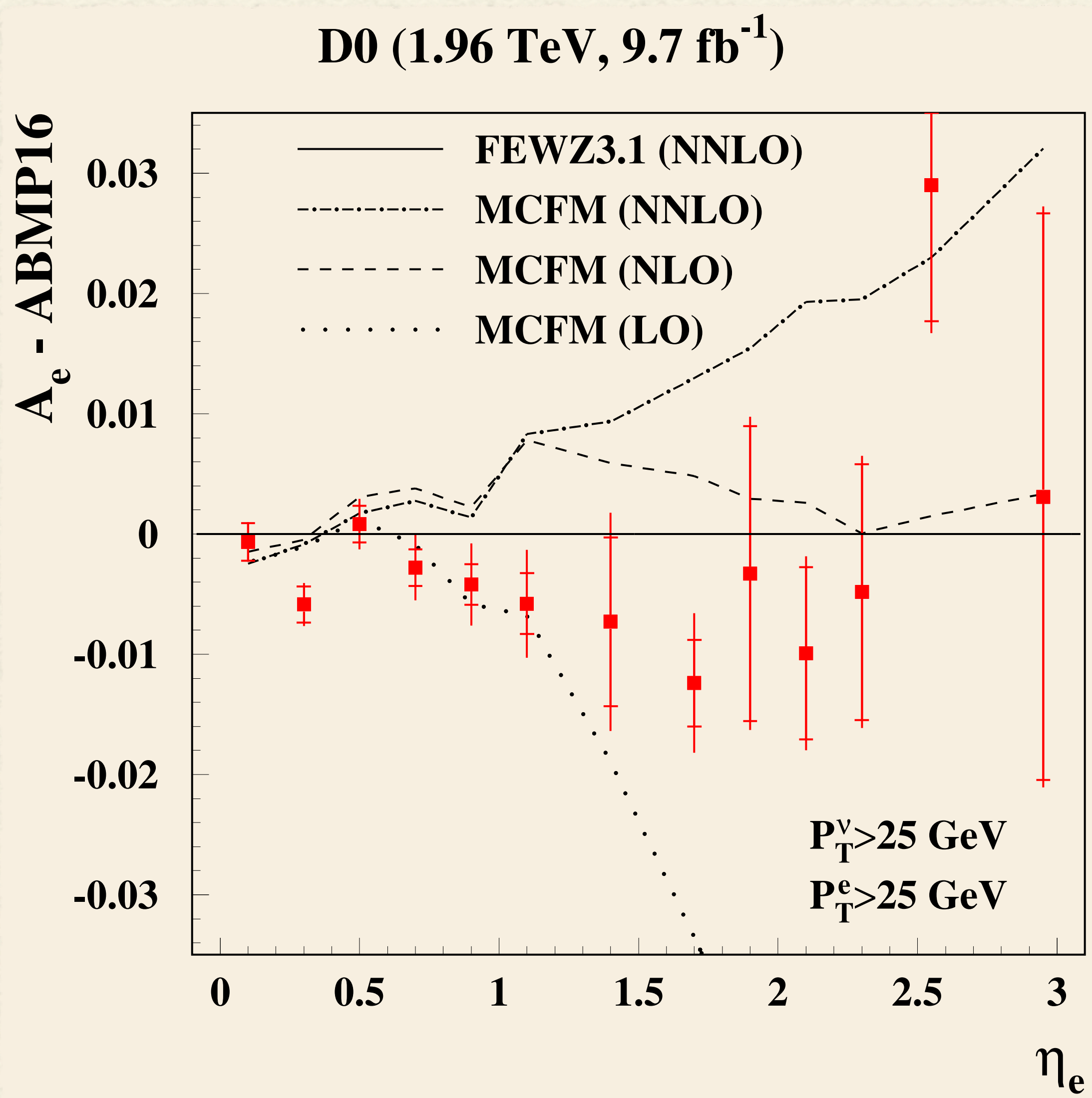

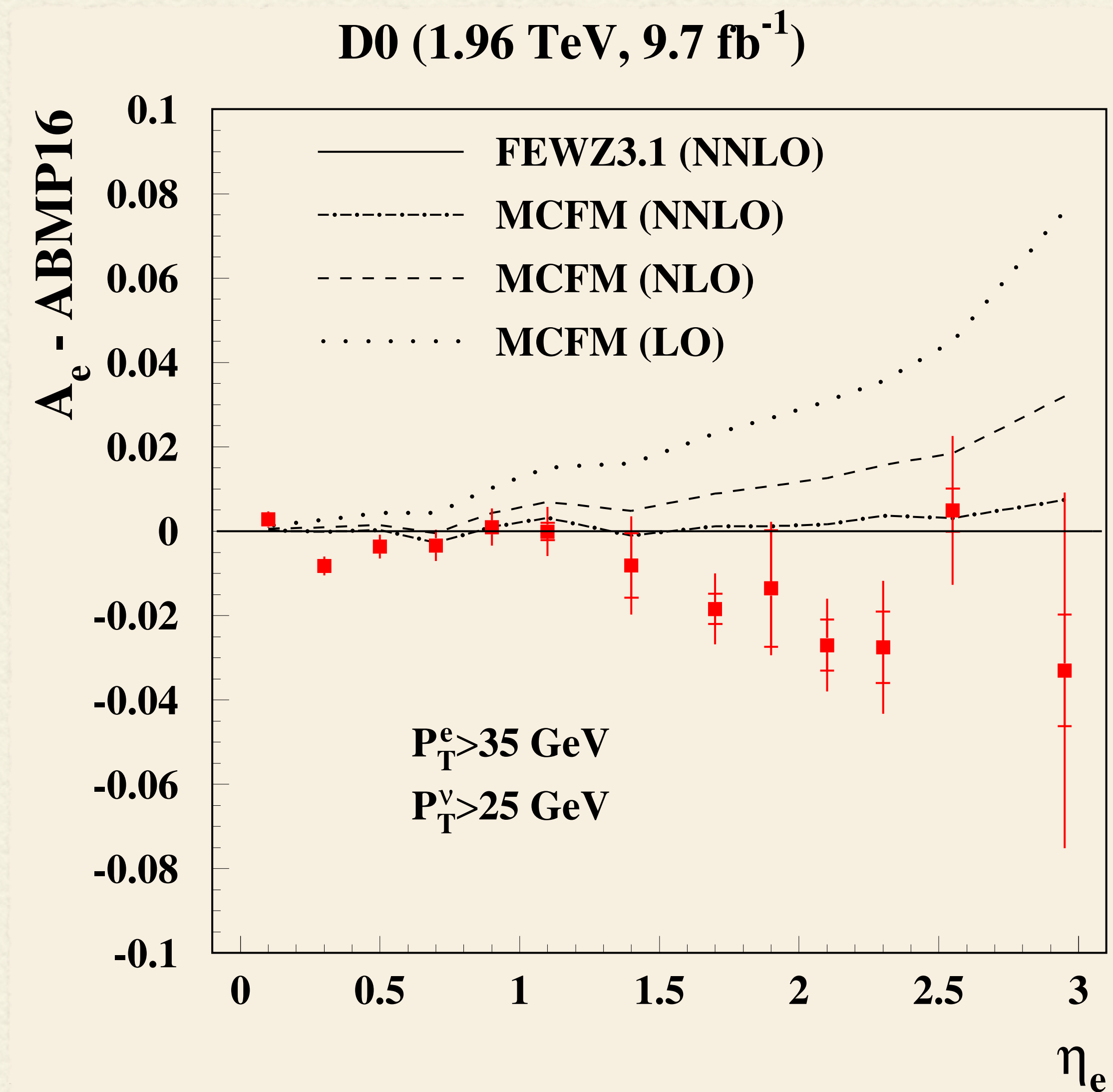

electron charge asymmetry distribution A_e in $W^\pm$ boson production at LO, NLO and NNLO normalized to **FEWZ** at NNLO

Left: symmetric cuts Right: staggered cuts as indicated in the plots